JOURNAL OF MAGNETIC RESONANCE **133,** 286–290 (1998)
ARTICLE NO. MN981468

Simple Two-Pulse Detection Scheme in Pulsed EPR for Studying Low-Frequency Nuclear Coherences

S. A. Dzuba,* I. V. Borovykh,† and A. J. Hoff†,[1]

**Institute of Chemical Kinetics and Combustion, Russian Academy of Sciences, 630090 Novosibirsk, Russia; and †Department of Biophysics, Huygens Laboratory, Leiden University, P.O. Box 9504, 2300 RA Leiden, The Netherlands*

Received December 22, 1997

A microwave two-pulse sequence with a weak and long 180° first pulse and a hard 90° second pulse is employed to detect nuclear coherences in pulsed EPR. The coherences created by the first pulse are transferred after an evolution period *T* into an observable FID by the second pulse. The free induction is measured at some fixed delay after the second pulse; it is modulated when *T* is varied. As the second pulse may be switched on immediately after the first pulse, the nuclear coherences may be detected immediately as they start to freely oscillate, without loss of information within the instrumental dead time. The method is demonstrated for a sample of the radical cation of ^{15}N-labeled bacteriochlorophyll *a*.

Key Words: **pulsed EPR; nuclear coherence; bacteriochlorophyll; dead time.**

INTRODUCTION

Electron spin echo envelope modulation (ESEEM) spectroscopy has proved to be a very efficient tool for studying electron–nuclear hyperfine interactions (*1, 2*). Modulation arises as a result of branching of different transitions excited simultaneously by the microwave pulse. There are basically two types of ESEEM experiment, the two-pulse (primary echo) and the three-pulse (stimulated echo). In the primary echo experiment, echo modulation appears because of interference between transitions of different frequencies. In the stimulated echo, the first two pulses create a coherence between nuclear states of the same electron spin manifold. This coherence is then transferred by the third pulse to the observable electron coherence. Many variations have been devised (*1, 2*), including two- and three-dimensional experiments (*3*).

The most serious drawback of the ESEEM modulation experiment is the instrumental dead time that is induced by cavity ringing after a microwave pulse. A loss of the initial time interval may be critical for broad lines, which are the rule in disordered systems, as the line shape is distorted substantially and therefore difficult to interpret. The distortion is especially prominent for the cosine and sine Fourier transforms (spectra of absorption and dispersion, respectively), because of the dead-time induced phase shifts, so normally only absolute value spectra are analyzed (*2*). To overcome this problem, different detection schemes have been proposed. We mention a 5-pulse sequence for the remote primary echo detection (*4*), a 7-pulse sequence for the remote HYSCORE echo detection (*3*), and a 4-pulse sequence employing a combination of selective and nonselective microwave pulses (*5*).

In the present work we propose a simple 2-pulse sequence which, on the one hand, allows detection of nuclear coherences of the same type as in the 3-pulse stimulated echo experiment but, on the other hand, is free from the instrumental dead time. Conceptually, the developed approach may be considered a hybrid of the coherent Raman beat detection of nuclear coherences suggested by Bowman (*6*) and of the FID-detected hole burning in pulsed EPR developed in Schweiger's group (*7, 8*).

The pulse scheme is shown in Fig. 1. Nuclear coherences are produced by the first weak and long microwave pulse, which is neither ''hard'' nor ''soft'' (*6*). The amplitude of this pulse is comparable with the parameters of the static spin Hamiltonian, so many nuclear transitions are excited (the pulse is not soft) but evolution during excitation depends not only on the pulse amplitude and duration but also on the Hamiltonian parameters (the pulse is not hard). The amplitude of the first pulse is also low enough that the second, a hard 90° pulse, creates an FID that is observable after the instrumental dead time imposed by the second pulse (*8*). (Normally the FID is obscured within the dead time because of the large inhomogeneous broadening of the EPR line. The hole burned by the low-amplitude pulse has a width approximately equal to the pulse (B_1) amplitude. Thus, for a 180° first pulse of duration t_D, the FID after the second pulse lasts approximately t_D also (*8*).) This FID, taken at some delay *t* after the second pulse, is measured as a function of the delay *T* between the two pulses. To avoid FID after the first pulse and unwanted echoes after the second pulse, the experiment is carried out twice, with the phase of the first pulse cycled between 0° and 180°, and the resulting signals added.

Note that similar pulse sequences, but with different detec-

[1] To whom correspondence should be addressed. Fax: (31) 71 5275819. E-mail: Hoff@rulhl1.LeidenUniv.nl.

1090-7807/98 $25.00

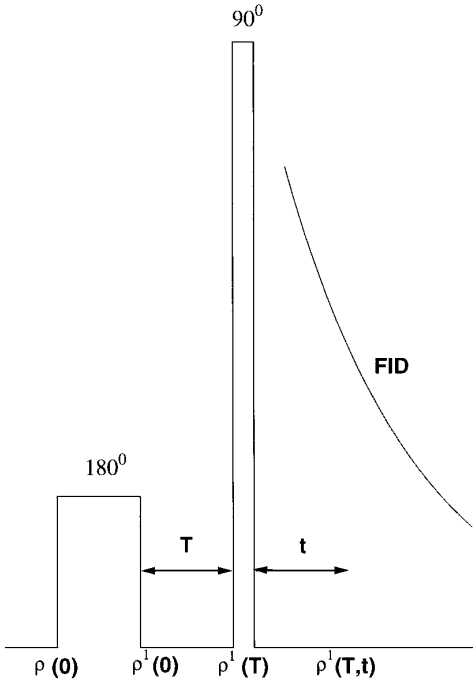

FIG. 1. Pulse sequence and measuring scheme employed. The first pulse is a weak 180° long pulse (~150 ns or longer). It produces nuclear coherences between energy sublevels. After the evolution period T the second, hard 90° pulse is applied, which transfers these coherences into an observable FID signal. This signal lasts beyond the spectrometer dead time because it belongs to the narrow hole burned in the spectrum by the first pulse. The FID is measured at some fixed delay t after the second pulse as a function of T. Also shown are the density matrix notations used in the text. The first pulse is cycled by 180° to avoid FID after the first pulse and unwanted echoes after the second pulse.

tion schemes and/or pulse amplitudes, and therefore with different type of information derived, have been employed in a number of previous ESEEM studies (*7–10*). Wacker and Schweiger (*7*), for example, studied the FID after the second pulse as a function of t when T was fixed and close to zero (see below). Earlier (*9, 10*), the echo signal appearing after the first long and weak pulse and the second short and strong pulse were studied.

THEORY

Let us consider a $S = \frac{1}{2}$, $I = \frac{1}{2}$ model system described by the rotating-frame Hamiltonian

$$H_0 = \Delta\omega S_Z + \omega_I I_Z + AS_Z I_Z + BS_Z I_X, \qquad [1]$$

where $\Delta\omega$ is the difference between the electron Zeeman frequency ω_0 and the microwave frequency ω, ω_I is the nuclear Zeeman frequency, A and B are determined by the elements of the hyperfine tensor, $A = T_{ZZ}$, $B = (T_{ZY}^2 + T_{ZX}^2)^{1/2}$. In the presence of the microwave field applied along the X axis of the rotating frame, Hamiltonian [1] is changed to

$$H_1 = H_0 + \omega_1 S_X, \qquad [2]$$

where ω_1 is the amplitude of the microwave frequency.

The density matrix changes according to

$$\rho(t) = \exp(-iHt)\rho(0)\exp(iHt), \qquad [3]$$

where H is given by [1] or [2], depending on whether the microwave field is applied or not. $\rho(0)$ is the initial density matrix; in thermal equilibrium it may be taken to be $\rho(0) = 1 - (\hbar\omega_0/kT)S_Z$.

Hamiltonian [1] is easily diagonalized, resulting in the energy levels

$$\begin{aligned} E_1 &= -\Delta\omega/2 - \omega_\beta/2 \\ E_2 &= -\Delta\omega/2 + \omega_\beta/2 \\ E_3 &= \Delta\omega/2 - \omega_\alpha/2 \\ E_4 &= \Delta\omega/2 + \omega_\alpha/2 \end{aligned} \qquad [4]$$

with the two nuclear transition frequencies

$$\begin{aligned} \omega_\alpha &= [(A/2 + \omega_I)^2 + (B/2)^2]^{1/2} \\ \omega_\beta &= [(A/2 - \omega_I)^2 + (B/2)^2]^{1/2}. \end{aligned} \qquad [5]$$

Hamiltonian [2] in its general form cannot be diagonalized analytically. The well-known exception is the case of an ideal hard pulse, when $\omega_1 \gg \Delta\omega$, A, B, ω_1. In this case the density matrix after the pulse $\rho^1(0)$ can be found easily using Eq. [3]. However, a hard pulse does not produce observable nuclear coherence (*1, 2*). In fact nuclear coherence after a single microwave pulse appears when the pulse amplitude ω_1 is of the same order of magnitude as the parameters of Hamiltonian [1]. Analytical solution for the density matrix under this condition is possible only for some special cases. Fortunately, for our purposes we do not need the exact values of all the density matrix elements after the first pulse. Indeed, diagonal elements of $\rho^1(T)$ do not depend on time T and will appear in the described experiment as a constant offset only. (These elements produce a modulation of the FID if the latter is recorded as a function of t (*7, 8*).) The elements of the FID that are responsible for the first-order electron coherence disappear after phase cycling (see above).

Thus, the only matrix elements which govern the observed signal are those responsible for the nuclear coherence, $\rho_{12}^1(0) = (\rho_{21}^1(0))^*$ and $\rho_{34}^1(0) = (\rho_{43}^1(0))^*$. After evolution during time T, they become

$$\rho^1_{ij}(T) = \rho^1_{ij}(0)\exp(-i\omega_{ij}T), \quad [6]$$

where $\omega_{ij} = E_i - E_j$.

One can calculate easily the matrix elements after the second 90° hard pulse and after the subsequent evolution period t. For the transverse M_Y magnetization,

$$\begin{aligned} M_Y(T, t) &= \mathrm{Tr}\{S_Y\rho^1(T, t)\} \\ &= M^0_Y + \sin\eta\,\sin(\Delta\omega t)\mathrm{Re}\{\sin(\omega_\alpha t/2) \\ &\quad \times \exp(i\omega_\beta t/2)\rho^1_{12}(0)\exp(i\omega_\beta T) \\ &\quad - \sin(\omega_\beta t/2)\exp(i\omega_\alpha t/2) \\ &\quad \times \rho^1_{34}(0)\exp(i\omega_\alpha T)\}, \end{aligned} \quad [7]$$

where M^0_Y is the T-independent fraction of FID coming from the diagonal elements of the density matrix $\rho^1(0)$ and η is the angle between two quantization axes for the nuclear spin [1],

$$\sin\eta = \omega_1 B/\omega_\alpha\omega_\beta. \quad [8]$$

Equation [7] must to be averaged over the distribution of the frequency offset $\Delta\omega$ arising from the inhomogeneous line broadening (determined by the width of the hole in our case). On first sight, M_y averages to zero because $\sin(\Delta\omega t)$ is an antisymmetric function of $\Delta\omega$. However, $\rho^1_{12}(0)$ and $\rho^1_{34}(0)$ may also be antisymmetric functions of $\Delta\omega$. This was shown explicitly for the weak coupling case (*6*) and may be qualitatively understood for the general case from the following argument. Nuclear coherence appears because, when the pulse is neither hard nor soft, magnetization is allowed to refocus during the nutation induced by this pulse. The same result would be obtained when two ideal hard pulses are applied separated by some interval τ for free precession (the first two pulses in a stimulated echo experiment). The resulting matrix elements may be readily found:

$$\begin{aligned} \rho^1_{12}(0) &\sim -\sin\eta\,\sin(\Delta\omega\tau)\sin(\omega_\alpha\tau/2)\exp(i\omega_\beta\tau/2) \\ \rho^1_{34}(0) &\sim \sin\eta\,\sin(\Delta\omega\tau)\sin(\omega_\beta\tau/2)\exp(i\omega_\alpha\tau/2). \end{aligned} \quad [9]$$

One can see that the two matrix elements are antisymmetric functions of $\Delta\omega$. Note also that the T-modulated part of the observable magnetization, according to [7] and [9], is proportional to $\sin^2\eta$, as in the usual ESEEM experiment.

Fourier transformation of Eq. [7] with respect to the time T directly provides nuclear transition frequencies ω_α and ω_β. As the second pulse may be switched on immediately after the first pulse is ended, the nuclear coherences may be detected immediately when, after the first pulse is ended, they start to freely oscillate. For long T delays, the signal is suppressed by spin–lattice relaxation.

Equation [7] predicts that the phases and amplitudes of the oscillations depend on three factors, $\sin(\omega_{\alpha(\beta)}t/2)$, $\exp(i\omega_{\beta(\alpha)}t/2)$, and $\rho^1_{12(34)}(0)$. The first factor may cause a suppression effect, which is common for the usual stimulated ESEEM experiment. To diminish its influence, one may make measurements at different delays t and then average the result (after calculating the absolute value spectrum). The averaging may be performed by summing all the spectra. The second factor is a phase-shifting factor, which may be eliminated by calculation of the absolute value spectrum of complex Fourier transformation. From another point of view, these two factors may help in assigning the lines in complicated spectra. Indeed, Eq. [7] may be Fourier transformed twice, with respect to the times T and t. The off-diagonal peaks in the resulting two-dimensional spectrum will show correlation between the coupled nuclear frequencies ω_α and ω_β—the same result as in the HYSCORE experiment (*3*). (The obvious obstacle in our approach is the dead-time problem of FID detection at small t and fast decay of FID when t is increased.)

Finally, the relative amplitudes and phases of the matrix elements $\rho^1_{12}(0)$ and $\rho^1_{34}(0)$ also must be taken into consideration. In some favorable cases, the relation between them may be very simple. Two such cases have been pointed out by Bowman (*6*). If hyperfine interaction is weak, $|\omega_I| > |A|$, then $\rho^1_{12}(0) = -\rho^1_{34}(0)$. The other case is a semiselective excitation, $\omega_\alpha \gg \omega_I \gg \omega_\beta$, when nuclear coherences are excited only within one electron spin manifold. Then $|\rho^1_{12}(0)| \gg |\rho^1_{34}(0)| = 0$. If the relation between the two elements is more complicated, this may also result in a suppression effect.

A general restriction of the approach we suggest is the relatively small total frequency range that may be investigated. This range is determined by the width of the hole burned by the first pulse. It cannot be made larger than 5–10 MHz, as otherwise the FID after the second pulse would be buried within the instrumental dead time. Therefore, our approach can be applied to low-frequency nuclear coherences only.

RESULTS

We studied, as an example, the radical cation of ^{15}N-labeled bacteriochlorophyll *a*.

Figure 2 shows examples of the acquired time traces, given for several chosen time delays t. As follows from Eq. [7], the observed signal has a nonmodulated contribution from M^0_Y. This contribution decays due to relaxation. The slowly decaying contribution to the signal was removed by exponential fitting of the tail and subsequent subtraction. The remaining fast decaying component (which is probably due to spectral diffusion) was removed by additional exponential fitting. The data was zero filled and complex Fourier transformation was performed.

The cosine, sine, and absolute value spectra for the delays chosen in Fig. 2 are shown in Fig. 3. One can see that the

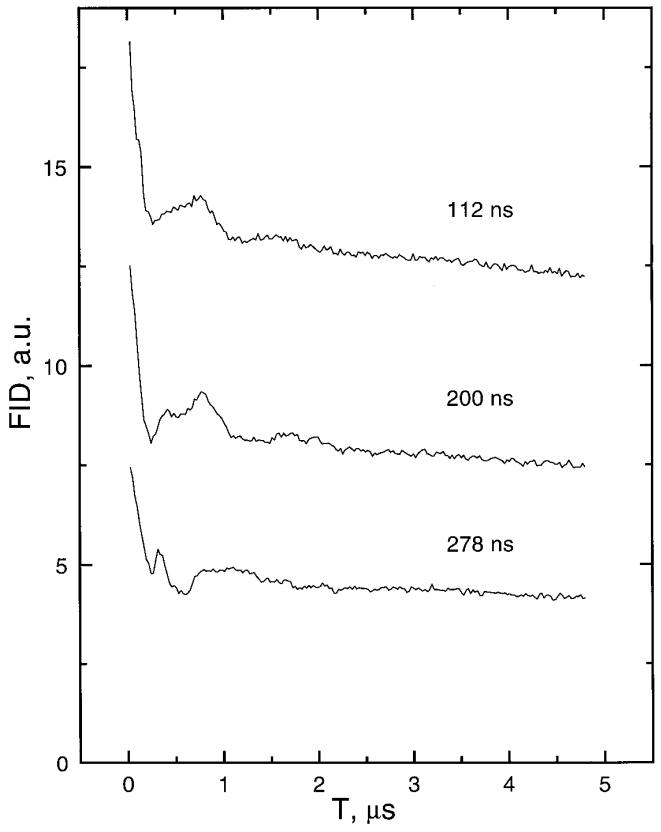

FIG. 2. Some selected time traces of the FID as a function of T (see Fig. 1) acquired for a sample of ^{15}N-labeled bacteriochlorophyll *a* radical cation. Temperature, 60 K; repetition frequency, 250 Hz; number of acquisitions, 200. Delays after the second pulse are indicated.

cosine and sine spectra contain relatively narrow lines, especially in the range 1–2 MHz. Figure 4 gives the result of averaging over time t by summing all the magnitude spectra (total number of spectra involved in the averaging is 25). The spectrum in Fig. 4 may be compared with data obtained in a usual stimulated ESEEM experiment (*11–14*). The most comprehensive study was performed in (*14*), where special care was taken to diminish the suppression effect. The spectrum in Fig. 4 has peak positions similar to those presented in (*14*), but is characterized by a better resolution at low frequency.

CONCLUSIONS

The results show that the suggested two-pulse measuring scheme possesses all the merits of the traditional three-pulse stimulated echo experiment. The only drawback is a limited range of frequencies (several MHz) that may be excited by the first pulse and therefore investigated. The obvious advantage is that the nuclear coherences may be detected without loss of any part of the time interval during which they evolve. This will restore the line shape of broad lines in disordered solids (limited again by the above frequency range) and allow one to obtain narrow peaks, especially for sine and cosine transforms. The latter property is important when detailed analysis of the line shape is needed, e.g., when employing nuclear transitions to study motional effects (*15*).

EXPERIMENTAL

Preparation of the ^{15}N-bacteriochlorophyll *a* sample is described elsewhere (*11*).

Measurements were carried out on a Bruker ESP 380 FT EPR spectrometer, with a dielectric cavity (Bruker ER 4118 X-MD-5) inside an Oxford Instruments CF 935 liquid-helium flow cryostat. The cavity Q value was adjusted to provide a spectrometer dead time of about 100 ns. Two microwave pulses were produced in different pulse-forming microwave units. The pulse widths were 296 ns for the first pulse and 16 ns for the second one. The microwave amplitudes of both pulses were adjusted to provide maximum FID amplitude after the second pulse. This choice implies that the first pulse is a 180° pulse and the second is a 90° pulse. (The pulse amplitudes are 1.7 and 15.6 MHz, respectively.) The phase was adjusted to provide maximum FID amplitude in one channel of the quadra-

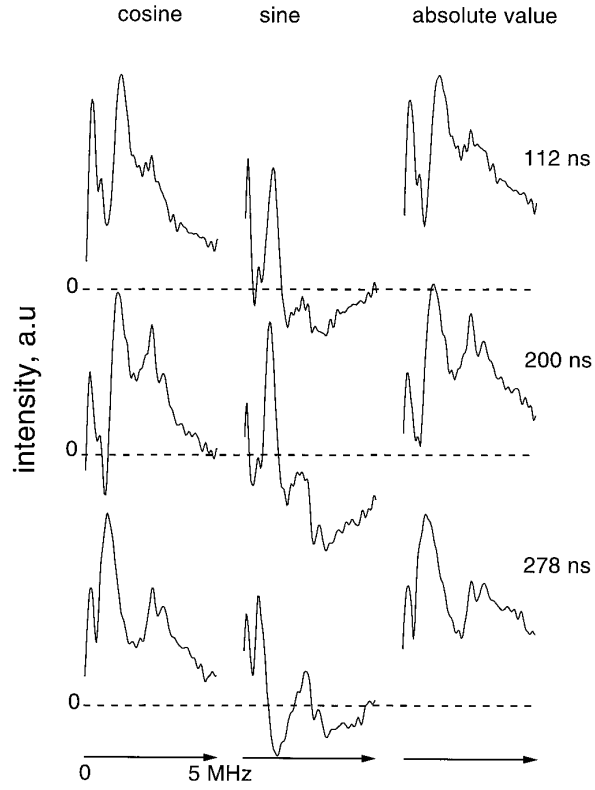

FIG. 3. Sine, cosine, and absolute value Fourier transforms of the time traces shown in Fig. 2. Prior to transformation, a two-exponential relaxation was subtracted (see text for details) and the data was zero filled.

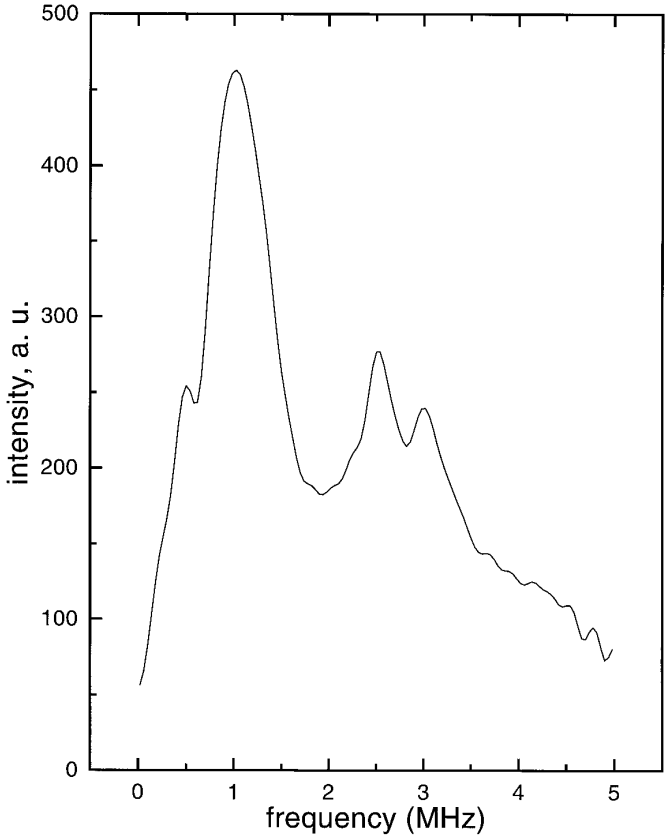

FIG. 4. The absolute value Fourier transform averaged for the time delays t after the second pulse ranging from 112 to 304 ns, with a step of 8 ns. The total number of acquisitions is 5000. The total acquisition time is 5.6 h.

ture detection, whereas in the other channel it was close to zero. FIDs were acquired using a sampling digitizer[2] at a fixed delay t after the second pulse, whereas the time separation T between the two pulses was varied between 0 and 4800 ns, with steps of 24 ns. The time delay t in different measurements was varied between 112 and 304 ns, with steps of 8 ns. The lower limit of t is determined by the dead time, and the upper limit is determined by signal decay. Analysis of the data was done on a personal computer, using homemade programs for data fitting and Fourier transformation.

[2] It is also possible to detect the FID by using a transient recorder (such as a LeCroy oscilloscope).

ACKNOWLEDGMENTS

The authors are grateful to Dr. M. K. Bowman for helpful discussion. This work was supported by the Foundation for Chemical Research (SON), financed by the Netherlands Organisation for Scientific Research (NWO). S.A.D. acknowledges Travel Grant 047-03-024 from NWO.

REFERENCES

1. A. Schweiger, *in* ''Modern Pulsed and Continuous-Wave Electron Spin Resonance Spectroscopy'' (L. Kevan and M. K. Bowman, Eds.), Wiley, New York (1990).
2. S. A. Dikanov and Yu. D. Tsvetkov, ''Electron Spin Echo Modulation (ESEEM) Spectroscopy,'' CRC Press, Boca Raton, FL (1992).
3. P. Hofer, *J. Magn. Reson. A* **111,** 77 (1994).
4. H. Cho, S. Pfenninger, G. Gemberle, A. Schweiger, and R. R. Ernst, *Chem. Phys. Lett.* **160,** 391 (1989).
5. J. Sebbach, E. C. Hoffman, and A. Schweiger, *J. Magn. Reson. A* **116,** 221 (1995).
6. M. K. Bowman, *Israel J. Chem.* **32,** 339 (1992).
7. Th. Wacker and A. Schweiger, *Chem. Phys. Lett.* **186,** 27 (1991).
8. Th. Wacker, G. A. Sierra, and A. Schweiger, *Israel J. Chem.* **32,** 305 (1992).
9. A. Schweiger, L. Braunschweiler, J.-M. Fauth, and R. R. Ernst, *Phys. Rev. Lett.* **54,** 1241 (1985).
10. L. Braunschweiler, A. Schweiger, J.-M. Fauth, and R. R. Ernst, *J. Magn. Reson.* **64,** 160 (1985).
11. A. J. Hoff, A. De Groot, S. A. Dikanov, A. V. Astashkin, and Yu. D. Tsvetkov, *Chem. Phys. Lett.* **118,** 40 (1985).
12. C. P. Lin, M. K. Bowman, and J. R. Norris, *J. Chem. Phys.* **85,** 56 (1986).
13. A. V. Astashkin, S. A. Dikanov, and Yu. D. Tsvetkov, *Chem. Phys. Lett.* **130,** 337 (1986).
14. H. Käss, J. Rautter, B. Bonigk, P. Hofer, and W. Lubitz, *J. Phys. Chem.* **99,** 436 (1995).
15. U. E. Nordh and N. P. Benetis, *Chem. Phys. Lett.* **244,** 321 (1995).